X-band inverse class-F GaN internally-matched power amplifier*

Bo-Chao Zhao(赵博超)[1], Yang Lu(卢阳)[1], Wen-Zhe Han(韩文哲)[1], Jia-Xin Zheng(郑佳欣)[2], Heng-Shuang Zhang(张恒爽)[1], Pei-jun Ma(马佩军)[1,†], Xiao-Hua Ma(马晓华)[2], and Yue Hao(郝跃)[1,2]

[1] *School of Microelectronics, Xidian University, Xi'an* 710071, *China*

[2] *School of Advanced Material and Nanotechnology, Xidian University, Xi'an* 710071, *China*

(Received 6 February 2016; revised manuscript received 27 May 2016; published online 2 August 2016)

An X-band inverse class-F power amplifier is realized by a 1-mm AlGaN/GaN high electron mobility transistor (HEMT). The intrinsic and parasitic components inside the transistor, especially output capacitor C_{ds}, influence the harmonic impedance heavily at the X-band, so compensation design is used for meeting the harmonic condition of inverse class-F on the current source plane. Experiment results show that, in the continuous-wave mode, the power amplifier achieves 61.7% power added efficiency (PAE), which is 16.3% higher than the class-AB power amplifier realized by the same kind of HEMT. To the best of our knowledge, this is the first inverse class-F GaN internally-matched power amplifier, and the PAE is quite high at the X-band.

Keywords: GaN internally-matched power amplifier, inverse class-F, compensation design, X-band power amplifier

PACS: 73.61.Ey, 84.60.Bk, 84.30.Le, 84.40.–x **DOI:** 10.1088/1674-1056/25/9/097306

1. Introduction

GaN high electron mobility transistors (HEMTs) have advantages in breakdown voltage, power density, and high electron, so they are good choices for high-frequency high-efficiency power amplifiers.[1–3] Smaller in size compared with a hybrid microwave integrated circuit (HMIC) and better in thermal performance compared with a monolithic microwave integrated circuit (MMIC), the internally-matched power amplifier is a competitor for C-band and X-band applications. Class-F and inverse class-F[4] are two important ways to improve power added efficiency (PAE) in design. Their principles are both that: output impedances at fundamental and harmonic frequencies are presented appropriately, so the output current and voltage waveforms are shaped to minimize the power dissipation and then more power is carried out.

Several high efficiency GaN-based power amplifiers have been presented. In 2009, Helaoui *et al.*[6] designed an L-band 81% PAE class-F power amplifier. In 2011, Kim *et al.*[7] manufactured S-band 69.9% PAE class-F and 69.4% PAE inverse class-F power amplifiers. We also increased the PAE of the GaN-based internally-matched power amplifier to 71% at 4 GHz[8] and 69% at 5.5 GHz.[9] At X-band applications, Resca *et al.*[10] reported a GaN MMIC power amplifier with 38% PAE for future generation synthetic aperture radar (SAR) systems. Waltereit *et al.*[13] developed a 50% PAE GaN MMIC with life times above 10^5 h for space applications. However, the power amplifier with PAE over 60% at the X-band is rarely seen because of the heavy parasitic effects.

In this paper, the compensation design of an X-band inverse class-F internally-matched power amplifier is used based on GaN HEMTs with 1-mm gate width. The second harmonic open and the third harmonic short are achieved on the current source plane. Under the continuous-wave condition, the amplifier achieves a high PAE of 61.7% at 8.1 GHz with an output power of 6.7 W. The rest of this paper is structured as follows: Section 2 introduces the basic principle of inverse class-F PA. The compensation design and simulation of the inverse class-F are shown in Section 3. Experiment results and comparisons with class-AB and other works are shown in Section 4. The conclusion is in Section 5.

2. Inverse class-F theory

An HEMT is essentially a voltage-controlled current source. Seen from the current source plane, the voltage and current waveforms of the ideal inverse class-F power amplifier are shown in Fig. 1 in solid lines. The waveforms of the current and the voltage are a square wave and a half sine wave, respectively, which have a phase difference of 180 degrees. At the first half period, the current is zero, so the dissipation power at the transistor is zero. While at the second half period, the voltage is zero, so the dissipation power at the transistor is zero as well. In theory, the drain efficiency will be 100% because no power is dissipated at the transistor and all of them are transmitted.

The next question is how to realize the waveform shown in Fig. 1. The Fourier expansion of the transistor drain current waveform is

$$I_{\rm d} = I_{\rm dc} - I_1\cos(wt) + I_3\cos(3wt)$$

*Project supported by the National High Technology Research and Development Program of China (Grant No. 2015AA016801).

†Corresponding author. E-mail: pjma@xidian.edu.cn

© 2016 Chinese Physical Society and IOP Publishing Ltd

$$-I_5\cos(5wt)+I_7\cos(7wt)+\cdots, \quad (1)$$

where I_{dc} is DC current, I_1, I_3, I_5, and I_7 are the fundamental and odd harmonic current amplitudes, and w is the angular frequency. The Fourier expansion of voltage waveform is

$$V_d = V_{dc}+V_1\cos(wt)+V_2\cos(2wt)-V_4\cos(4wt) +V_6\cos(6wt)+\cdots, \quad (2)$$

where V_{dc} is the DC component of voltage, and I_1, I_2, I_4, and I_6 are fundamental and even harmonic voltage amplitudes. It can be seen from Eq. (1) that the current has no even components, so the admittance of even third harmonics is zero, in other words, even harmonics should be open. It can be seen from Eq. (2) that the voltage has no odd components, so the impedance of the odd harmonic is zero, it means that the odd harmonic should be short. The waveform and harmonic impedance situation are opposite to a class-F power amplifier.[5]

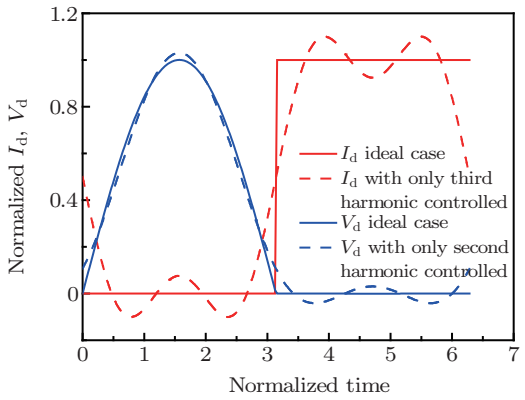


Fig. 1. (color online) Current and voltage waveforms of the inverse class-F PA in the ideal case and in the case when only the second and the third harmonics are controlled, respectively.

Generally, only the second and third harmonics are controlled in inverse class-F design, as it is very complex and there is less contribution to efficiency to control the harmonics with an order higher than third. The waveform under this condition is shown in Fig. 1 in dash lines. The key point to design an inverse class-F power amplifier is the second harmonic open, the third harmonic short, and the fundamental matching on the current source plane.

3. Amplifier design

3.1. Inverse class-F power amplifier at X-band

The 1-mm gate width GaN HEMT was fabricated at Xidian University, China.[9] The basic model is shown in Fig. 2. The equivalent circuit of GaN HEMT die is in the red box consisting of six parasitic parameters and seven intrinsic parameters. Here, "B" is the drain pad plane on which an impedance matching network is usually designed. "A" is the current source plane where the harmonic impedance condition should be met.

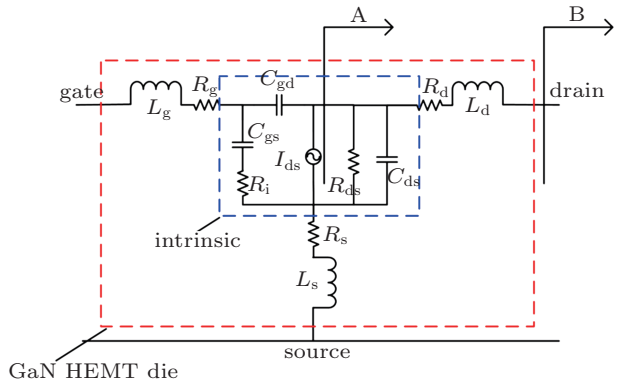


Fig. 2. (color online) Typical GaN HEMT model. "B" is the drain pad plane and "A" is the current source plane.

It is assumed that the inverse class-F impedance condition where the second harmonic open and the third harmonic short are realized on plane "B", figure 3 shows what they will be on plane "A". Due to drain parasitic inductance L_d, drain parasitic resistance R_d, drain source resistance R_{ds}, especially drain source capacitance C_{ds} (about 0.5 pF), the ideal impedance will change. The impedance has few changes at fundamental frequency under 4 GHz so the traditional design method that the second harmonic open and third harmonic short on plane "B" can been used as usual. However, the impedance changes largely at a fundamental frequency higher than the X-band so the compensation design must be considered. Meanwhile, C_{ds} influences the third harmonic more heavily than the second harmonic, and it is beneficial to the third harmonic short, so the inverse class-F power amplifier is easier to realize than the class-F power amplifier.

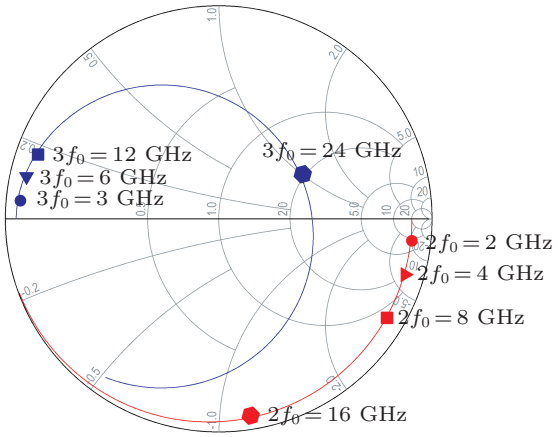


Fig. 3. (color online) The second and third harmonic impedance on plane "A" (shown in Fig. 2), when the second harmonic open and the third harmonic short on plane "B" at different frequencies.

3.2. Compensation design and simulation

The schematic structure of the output harmonic control network and fundamental matching network is shown in Fig. 4. TL_2 is an open ended shunt stub with length of 45 degrees. For the second harmonic, TL_2 is 90 degree and it transforms the impedance from open point A to short point B, so the

circuit at the right side of point B has no influence to the second harmonic. One transmission line (TL_1) and three parallel bonding wires (BW_1) are used for compensating the influence of components inside the GaN HEMT die. They also transform the impedance from short point B to open point C for second harmonic. The length of BW_1 (L_BW_1) tunes mainly for the second harmonic. TL_3 and BW_2 compensate the third harmonic, and transform the impedance to short at point C. The length of BW_2 (L_BW_2) tunes mainly for the third harmonic. The following fundamental matching network is used for matching the fundamental impedance to 50 Ω. The parameters of the matching network are shown in detail in Fig. 4.

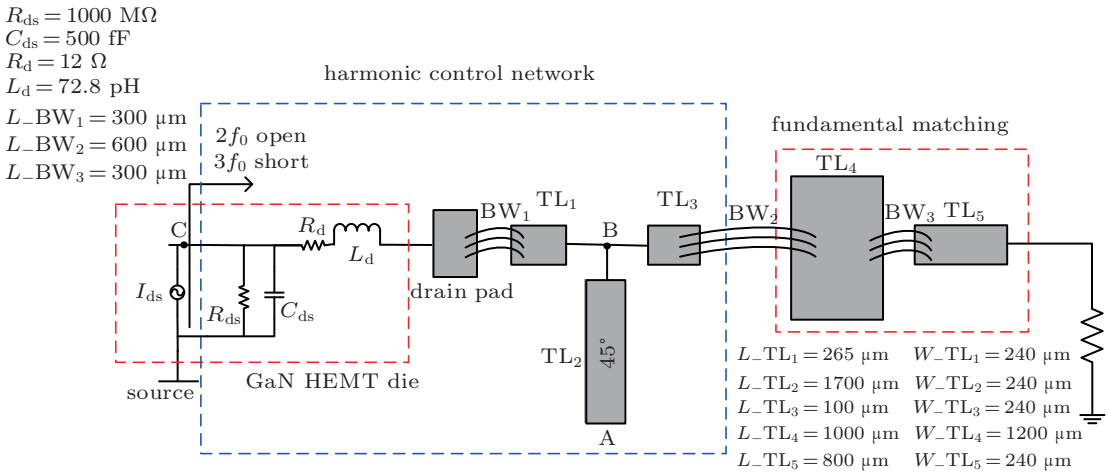


Fig. 4. (color online) Output harmonic control network and fundamental matching network. Second harmonic open and third harmonic short are achieved on the current source plane.

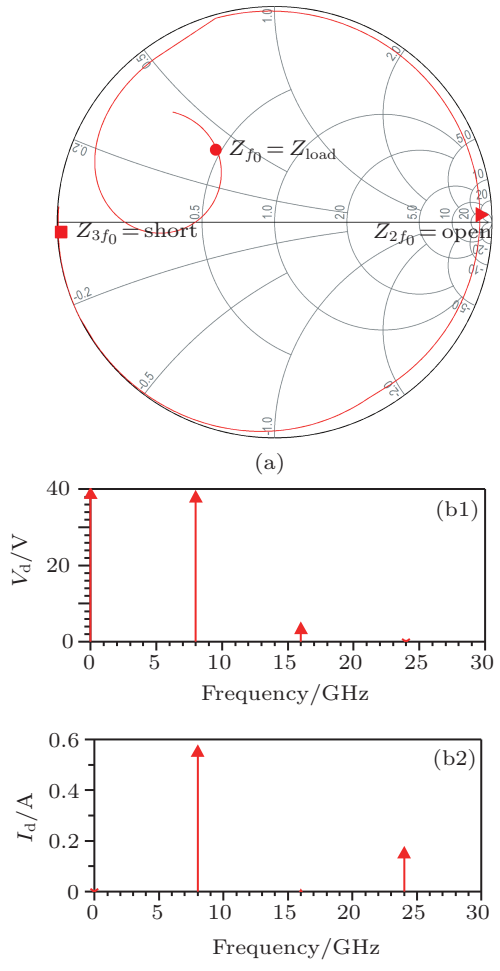


Fig. 5. (color online) Fundamental, second, and third harmonic impedance on the current source plane (a). Frequency spectrum of voltage (b1) and current (b2) on the current source plane.

The simulated impedance is shown in Fig. 5(a). Seen from the current source plane, the second harmonic is open while the third harmonic is short, the fundamental impedance equals to the load impedance obtained from the loadpull simulation. The desired inverse class-F load condition is obtained. In terms of input, a transmission line, a high dielectric ceramic capacitor, and bonding wires achieve the matching. The entire circuit schematic is simulated using an ADS Harmonic–Balance simulator. In the frequency domain, the simulate frequency spectrum is shown in Fig. 5(b). The voltage has the DC component, fundamental component, and second harmonic component, while the current has the fundamental component and the third harmonic component. In the time domain, the current and voltage waveforms seen from the current source plane are shown in Fig. 6. The voltage is close to a half sine wave while the current is approaching a square wave, and the overlap of voltage and current is reduced. This indicates an explicit inverse class-F power amplifier of the X-band.

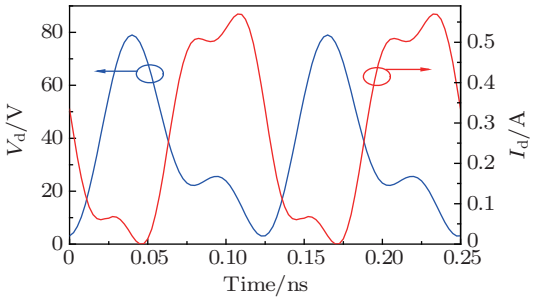


Fig. 6. (color online) Simulated waveforms of current and voltage on the current source plane.

4. Realization and performance

The matching modules are soldered in a package with a cavity size of 14.5 mm×14.8 mm. The 1-mil (1 mil = 0.0254 mm) diameter bonding wires connect the modules, participating in the match at the same time. Due to the manufacturing error and model error, the lengths of BW_1 and BW_2 can tune the second and third harmonics respectively (the MMIC power amplifier cannot be tuned after being fabricated). The photograph of the proposed X-band inverse class-F power amplifier is shown in Fig. 7(a). For comparison, another X-band class-AB power amplifier where only the fundamental is matched and realized by the same kind of HEMT is shown in Fig. 7(b).

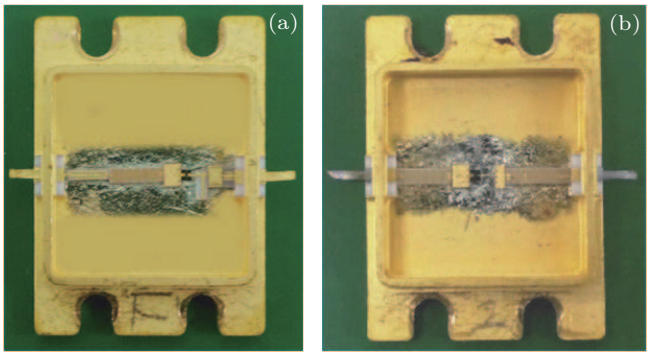


Fig. 7. (color online) Photographs of the proposed X-band inverse class-F power amplifier (a) and the compared X-band class-AB power amplifier (b).

The two power amplifiers are measured under the continuous-wave operation. The DC bias condition is V_{DS} = 40 V and I_{DS} = 60 mA. As described in Fig. 8, a 61.7% PAE is obtained when the input power P_{in} is pushed up to 26 dBm at the frequency of 8.1 GHz. The output power P_{out} is 6.7 W with a power gain of 12 dB. Compared with the class-AB power amplifier where the fundamental impedance is matched only, output power and gain are almost the same, while PAE of the proposed inverse class-F is 16.3% higher.

The frequency response of the two power amplifiers is also shown in Fig. 9. With almost the same output power and gain, the inverse class-F power amplifier has over 50% PAE, higher than the class-AB power amplifier from 7.7 GHz to 8.5 GHz. The second and third harmonics are controlled at a frequency of 8 GHz and they are more sensitive than the fundamental wave, so the PAE of the inverse class-F power amplifier has a relative narrow bandwidth than the class-AB power amplifier.

As a power amplifier product, the last process is parallel seam sealing to achieve high quality and long term reliability. After the sealing process, the variation of gain and PAE is less than 0.1 dB and 0.2%.

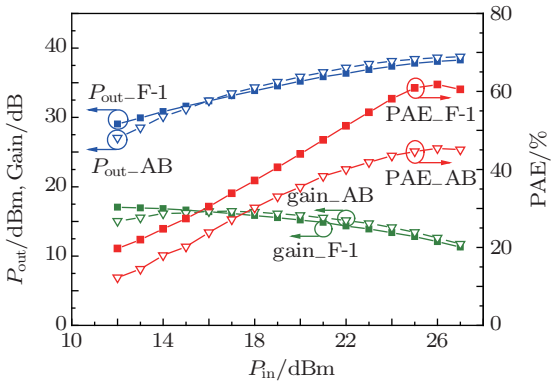


Fig. 8. (color online) Measured microwave performance of the power amplifier in continuous mode at 8.1 GHz. The output power P_{out}, gain, and PAE are compared between inverse class-F and class-AB power amplifiers.

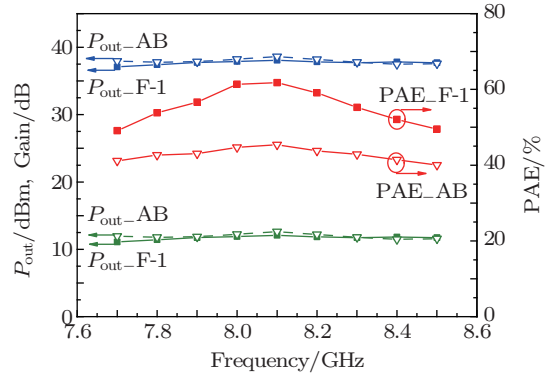


Fig. 9. (color online) Measured microwave performance of the power amplifier in continuous mode when input power is 26 dBm. The P_{out}, gain, and PAE are compared between inverse class-F and class-AB power amplifiers.

The comparison between the proposed inverse class-F power amplifier and other works is shown in Table 1. At low frequency, L-band to C-band, PAE can be increased over 70%, but the power amplifier at the X-band with PAE higher than 60% is barely seen, which may be caused by the increase of the drain source capacitance and parasitic resistance. It can also be seen from Table 1 that the proposed inverse class-F power amplifier has a high power density and high PAE at the X-band in continuous-wave mode.

Table 1. The high efficiency power amplifier at different frequency bands.

Ref.	Frequency band	Power density/(W/mm)	PAE/%	Mode[a]
this work	X-band	6.7	61.7	CW
[14]	X-band	3.25	44	CW
[13]	X-band	5	50	CW
[12]	X-band	4.6	48	CW
[11]	X-band	14.2	48	PW
[10]	X-band	3.5	38	PW
[9]	C-band	6.8	69.4	PW
[8]	C-band	8.5	71	PW
[7]	S-band	10	69.9	CW
[6]	L-band	10	81.3	CW

[a]CW is the continuous-wave mode and PW is the pulse wave mode.

Two-tone measurements are also performed to characterize the linearity of the inverse class-F power amplifier. As

shown in Fig. 10, the blue line represents the output power at a fundamental frequency of $f_1 = 8.05$ GHz while the red line represents the IM3 (3^{rd}-order two tone intermodulation product) at a frequency of $2f_2-f_1 = 8.25$ GHz. At the linear region, when the input power is 18 dBm, IMD3 (difference between the output power and IM3) is 31 dBc, indicating good linearity. At the saturation region, when the input power is pushed to 27 dBm, IMD3 is 20 dBc. OIP3 (output two tone the third-order intercept point) is determined by extrapolating the pout and IM3 curve. The point of intersection is OIP3 of 48 dBm.

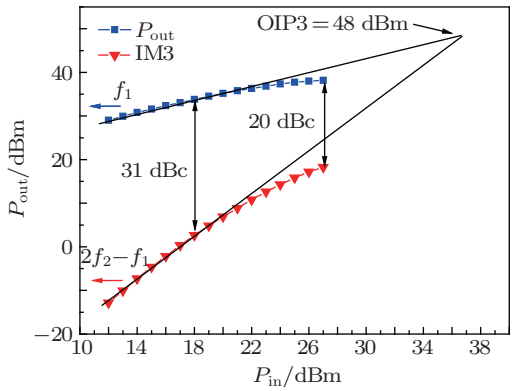


Fig. 10. (color online) Measured linearity performance using two-tone signal. Here, $f_1 = 8.05$ GHz and $f_2 = 8.15$ GHz.

5. Conclusion

An X-band 61.7% PAE inverse class-F power amplifier is presented. A harmonic control network is used for compensating the components inside the transistor model, so the inverse class-F impedance condition is obtained on the current source plane. The harmonic impedance can be tuned by the bonding wires (BW_1, BW_2) and the compensation design can also be used in large gate width HEMT internally-matched power amplifiers. To the best of our knowledge, this is the first inverse class-F GaN internally-matched power amplifier, and the PAE is relatively high in X-band applications.

References

[1] Yang P, Lv Y W and Wang X B 2015 *Acta Phys. Sin.* **64** 197303 (in Chinese)
[2] Guo R H, Lu T P, Jia Z G, Shang L, Zhang H, Wang R, Zhai G M and Xu B S 2015 *Acta Phys. Sin.* **64** 127305 (in Chinese)
[3] Lv Y J, Feng Z H, Gu G D, Yin J Y, Fang Y L, Wang Y G, Tan X, Zhou X Y, Lin Z J, Ji Z W and Cai S J 2015 *Chin. Phys. B* **24** 087306
[4] Cripps S C 2006 *RF Power Amplifiers for Wireless Communications* (2nd edn.) (London: Artech House) pp. 143–149
[5] Zhao B C, Lu Y, Wei J X, Dong L, Wang Y, Cao M Y, Ma X H and Hao Y 2015 *Chin. Phys. B* **24** 058401
[6] Helaoui M and Ghannouchi F M 2009 *IEEE Trans. Microw. Theory Tech.* **57** 314
[7] Kim J H, Jo G D, Oh J H, K Y H, Lee K C and Jung J H 2011 *IEEE Trans. Microw. Theory Tech.* **59** 153
[8] Lu Y, Cao M Y, Wei J X, Zhao B C, Ma X H and Hao Y 2014 *Electron. Lett.* **50** 1207
[9] Ma X H, Wei J X, Cao M Y, Lu Y, Zhao B C, Dong L, Wang Y and Hao Y 2014 *Chin. Phys. Lett.* **31** 108401
[10] Resca D, Raffo A, Falco S D, Scappaviva F, Vadala V and Vannini G 2014 *IEEE Microw. Wireless Compon. Lett.* **24** 266
[11] Peng M Z, Zheng Y K, Luo W J and Liu X Y 2011 *Solid State Electron.* **64** 63
[12] Barisich G C, Ulusoy A C, Gebara E and Papapolymerou J 2015 *IEEE Microw. Wireless Compon. Lett.* **25** 811
[13] Waltereit P, Kuhn J, Quay R, Raay F V, Dammann M, Casar M, Muller S, Mikulla M, Ambacher O, Latti J, Rostewitz M, Hirche K and Daubler J 2012 *Proceedings of the 7th European Microwave Integrated Circuits Conference,* October 29–30, 2012, Amsterdam, The Netherlands, pp. 123–126
[14] Barisich G C, Pavlidis S, Morcillo C A D, Chlieh O L, Papapolymerou J and Gebara E 2013 *IEEE International Conference on Microwaves, Communications, Antennas and Electronic Systems*, October 21–23, 2013, Tel Aviv, Israel